



Assessing the Feasibility of an Explicit Numerical Model for Simulating Water Surface Profiles over Weirs

Wesam S. Mohammed-Ali^{1*}, Esraa H. Khaleel²

¹ Department of Environmental Engineering, College of Engineering, Tikrit University, Tikrit 34001, Iraq

² Department of Mathematics, College of Computer Science and Mathematics, Tikrit University, Tikrit 34001, Iraq

Corresponding Author Email: wsm27f@mst.edu

<https://doi.org/10.18280/mmep.100337>

ABSTRACT

Received: 4 March 2023

Accepted: 10 May 2023

Keywords:

numerical modelling, water surface profile, HEC-RAS model, numerical simulation, finite difference equation

Investigating and managing water surface profiles over obstructions in waterways is a critical aspect of water resources engineering. To address this challenge, numerous studies have been conducted, emphasizing the importance of controlling water surface variations along waterways. This study evaluates the feasibility of employing an explicit numerical model to simulate the water surface profile over a V-notch weir. Experimentally, the water surface profile was measured for flow rates ranging from 10 to 70 liters per second. An explicit numerical solution for the water surface profile was developed based on the four-point box partial differential equation principle. The Nash-Sutcliffe Efficiency (NSE) was calculated to assess the agreement between the experimental and numerical results. With an average NSE value of 0.975, the proposed explicit numerical model demonstrated a high level of convergence with experimental measurements, indicating its potential for accurately simulating water levels above the weir.

1. INTRODUCTION

The water surface profile is a critical characteristic of open channel flow. In these waterways, various obstacles may influence the water surface profile, making it essential to understand the flow behavior as it traverses the waterway. Weirs are among the most common flow measurement instruments installed across the width of waterways or streams, significantly impacting the water surface profile. Numerous mathematical and empirical studies have investigated the prediction and measurement of the water surface profile over weirs, each yielding specific findings due to their limitations and boundary conditions.

Experimental and numerical investigations have been conducted to examine the stage-discharge relationship through rectangular sharp-crested weirs. By comparing different data sets with a statistical model, the numerical approach demonstrated acceptable agreement in replicating the flow behavior over rectangular sharp-crested weirs [1]. Additionally, a numerical study was developed to measure the flow over triangular and trapezoidal weirs during free-flow conditions, finding that the numerical model using nonlinear regression analysis closely matched the flow characteristics [2].

The flow pattern over an elliptical weir was investigated by establishing a regression analysis of the parameters influencing the flow regime. The results showed that, in addition to the short and long radius, the crest height ratio to the flow depth in front of the weir significantly impacts the water surface profile [3]. Several studies have also examined the flow characteristics of labyrinth weirs, both experimentally and theoretically. One study found that the flow ratio to crest height influences the water surface profile, with a reduced

impact when this ratio increases [4]. Other research confirmed that the length magnification or head-to-width ratio affects the flow pattern over a triangular labyrinth weir [5, 6].

As part of the flow characteristics analysis, the water surface profile over a triangular labyrinth weir was simulated using the volume of fluids methodology [7]. Solution uncertainty was determined using the Grid Convergence Index (GCI), and the volume of fluids results were compared to experimental work, showing an acceptable agreement from a practical perspective [8].

Several studies have focused on the flow over the broad-crested weir, investigating flow characteristics experimentally [9], through parametric studies using dimensional analysis [10, 11], and employing relaxation techniques [12]. Further investigations have addressed the impact of dimensions or shapes of a broad-crested weir on flow behavior in open channels [13, 14].

A review of the existing literature reveals considerable scientific efforts to study flow behavior over weirs due to their importance in water resource management. In this research, further investigation will be undertaken to assess the feasibility of employing a numerical model for calculating and estimating the water surface profile over a V-notch weir.

2. NUMERICAL SOLUTION METHODOLOGY

The Saint-Venant Equation represents the mass and momentum conservation principle of flow in natural streams and rivers. Solving the Saint-Venant numerically, including all the relevant characteristics, was explained in several well-known scientific articles [15-18]. However, the control volume of flow shown in Figure 1 includes the inflow, outflow,

and change in storage over time (t). Furthermore, in open channels, the (Δx) can be considered a small value; thus, the continuity equation can be numerically represented and written as shown in Eq. (1), where (A) is the cross-section area of the control volume.

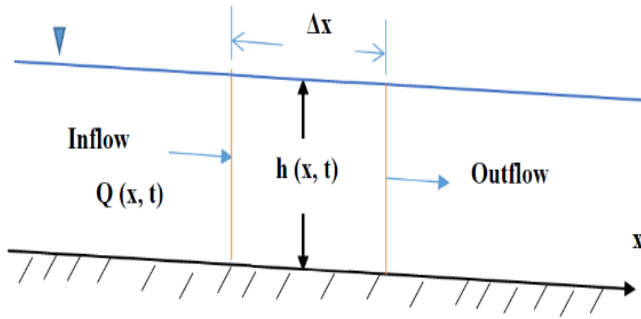


Figure 1. Continuity and momentum control volume

$$\frac{\partial Q}{\partial x} + \frac{\partial A}{\partial t} = 0 \quad (1)$$

Likes that the momentum equation is presented herein for the control volume, as shown in Eq. (2), where (g) is the acceleration due to gravity, (S_o) and (S_f) is the bed slope and water surface slope, respectively.

$$\frac{1}{A} \frac{\partial Q}{\partial t} + \frac{1}{A} \frac{\partial}{\partial x} \left(\frac{Q^2}{A} \right) + g \frac{\partial y}{\partial x} - g(S_o - S_f) = 0 \quad (2)$$

Bernoulli's Equation is utilized to predict the water surface profile in waterways subjected to gravity flow [19]. Bernoulli's Equation for the flow of fluid through the control volume can be written as shown in Eq. (3), in which (Z) is the bed elevation; (y) is the depth of water; (V) is the velocity of flow, and (h_t) is the loss of energy between the inflow section (1) and outflow section (2).

$$Z_1 + y_1 + \frac{V_1^2}{2g} = Z_2 + y_2 + \frac{V_2^2}{2g} + h_t \quad (3)$$

The implicit finite difference method is one of the most credible techniques for solving partial differential equations problems [20, 21]. The time-distance (x - t) grid shown in Figure 2 represents the scheme for solving the derivative parameters included in Eq. (1), Eq. (2), and Eq. (3). The solution will proceed simultaneously from the time step to the next time step along the distance.

The derivative of the equations as mentioned earlier (1) and (2) over distance can be shown in the following shape in Eq. (4) and (5), respectively, where ϕ is the distance weight parameter.

$$\frac{\partial Q}{\partial x} = \phi \left(\frac{Q_{i+1}^{j+1} - Q_i^{j+1}}{\Delta x_{i+1/2}} \right) + (1 - \phi) \left(\frac{Q_{i+1}^j - Q_i^j}{\Delta x_{i+1/2}} \right) \quad (4)$$

$$\frac{\partial}{\partial x} \left(\frac{Q^2}{A} \right) = \phi \left(\frac{\left(\frac{Q^2}{A} \right)_{i+1}^{j+1} - \left(\frac{Q^2}{A} \right)_i^{j+1}}{\Delta x_{i+1/2}} \right) + (1 - \phi) \left(\frac{\left(\frac{Q^2}{A} \right)_{i+1}^j - \left(\frac{Q^2}{A} \right)_i^j}{\Delta x_{i+1/2}} \right) \quad (5)$$

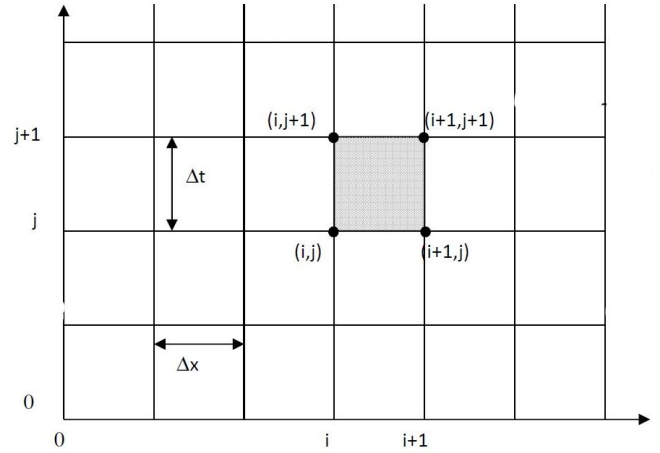


Figure 2. The implicit finite difference time-distance grid

While the derivative over time for Eqns. (1) and (2) is shown in Eq. (6) and Eq. (7), respectively.

$$\frac{\partial A}{\partial t} = 0.5 \left(\frac{A_{i+1}^{j+1} - A_{i+1}^j}{\Delta t^j} \right) + 0.5 \left(\frac{A_i^{j+1} - A_i^j}{\Delta t^j} \right) \quad (6)$$

$$\frac{\partial Q}{\partial t} = 0.5 \left(\frac{Q_{i+1}^{j+1} - Q_{i+1}^j}{\Delta t^j} \right) + 0.5 \left(\frac{Q_i^{j+1} - Q_i^j}{\Delta t^j} \right) \quad (7)$$

Furthermore, constant terms shown in Eq. (1) and Eq. (2) can be represented as expressed below,

$$S_f = \phi S_{f_{i+1/2}}^{j+1} + (1 - \phi) S_{f_{i+1/2}}^j \quad (8)$$

$$S_o = \phi S_{o_{i+1/2}}^{j+1} + (1 - \phi) S_{o_{i+1/2}}^j \quad (9)$$

$$A = \phi \left(\frac{A_{i+1}^{j+1} + A_i^{j+1}}{2} \right) + (1 - \phi) \left(\frac{A_{i+1}^j + A_i^j}{2} \right) \quad (10)$$

Finally, substituting the derived forms and constants in continuity Eq. (1) and the momentum Eq. (2) will lead to the final shape of these equations as shown in Eq. (11) and Eq. (12) respectively,

$$\phi(Q_{i+1}^{j+1} - Q_i^{j+1}) + (1 - \phi)(Q_{i+1}^j - Q_i^j) + \frac{\Delta x_{i+1/2}}{2\Delta t^j} (A_{i+1}^{j+1} - A_{i+1}^j + A_i^{j+1} - A_i^j) = 0 \quad (11)$$

$$\frac{1}{\phi \left(\frac{A_{i+1}^{j+1} + A_i^{j+1}}{2} \right) + (1 - \phi) \left(\frac{A_{i+1}^j + A_i^j}{2} \right)} \left[\left(0.5 \left(\frac{Q_{i+1}^{j+1} - Q_{i+1}^j}{\Delta t^j} \right) + 0.5 \left(\frac{Q_i^{j+1} - Q_i^j}{\Delta t^j} \right) \right) + \frac{1}{\phi \left(\frac{A_{i+1}^{j+1} + A_i^{j+1}}{2} \right) + (1 - \phi) \left(\frac{A_{i+1}^j + A_i^j}{2} \right)} \left[\left(\phi \left(\frac{\left(\frac{Q^2}{A} \right)_{i+1}^{j+1} - \left(\frac{Q^2}{A} \right)_i^{j+1}}{\Delta x_{i+1/2}} \right) + (1 - \phi) \left(\frac{\left(\frac{Q^2}{A} \right)_{i+1}^j - \left(\frac{Q^2}{A} \right)_i^j}{\Delta x_{i+1/2}} \right) \right) + g \left[\phi \left(\frac{h_{i+1}^{j+1} - h_i^{j+1}}{\Delta x_{i+1/2}} \right) + (1 - \phi) \left(\frac{h_{i+1}^j - h_i^j}{\Delta x_{i+1/2}} \right) \right] - g \left[\left(\phi S_{o_{i+1/2}}^{j+1} + (1 - \phi) S_{o_{i+1/2}}^j \right) - \left(\phi S_{f_{i+1/2}}^{j+1} + (1 - \phi) S_{f_{i+1/2}}^j \right) \right] \right] = 0 \quad (12)$$

The elements that have subscript time step (j) in the Continuity Eq. (11), and Momentum equation, Eq. (12), are already known either from the boundary condition or from the previous step of the Saint-Venant equation solution. Also, the cross-section area (A) is a water depth (h) function. Therefore, the only missing or unknown elements are the flow discharge (Q) and water depth (h) for the next time step (j+1) at both nodes (i) and (i+1). However, besides the initial and boundary condition, the final forms of the continuity equation and momentum equation can be utilized for simultaneously estimating the value of discharge and flow depth.

Speaking of which boundary condition status for the flow in open channels, the boundary condition upstream of the flow regime can be considered either the flow hydrograph (Q) or stage hydrograph (h) during the simulation time. It is also possible to adopt the values of the flow hydrograph (Q) or stage hydrograph (h) downstream of the flow regime, but it is possible to consider either a looped or single rating curve and critical depth of flow for this purpose.

3. EXPERIMENTAL TESTS

Numerous laboratory measurements were made of a range of flow discharges over a V-notch Triangular weir. Figure 3 shows the laboratory system utilized during this study and the setup during the running of the test.

The flow feeder was connected to an ultrasonic flow meter that can measure and read the discharge value upstream of the weir over time. Also, the gauge pointer was used to read the flow depth before and after the weir at a certain distance. These gage readings help to get the shape of the water surface profile over the weir. Table 1 lists the range of discharge that was used during the experimental portion of this study.

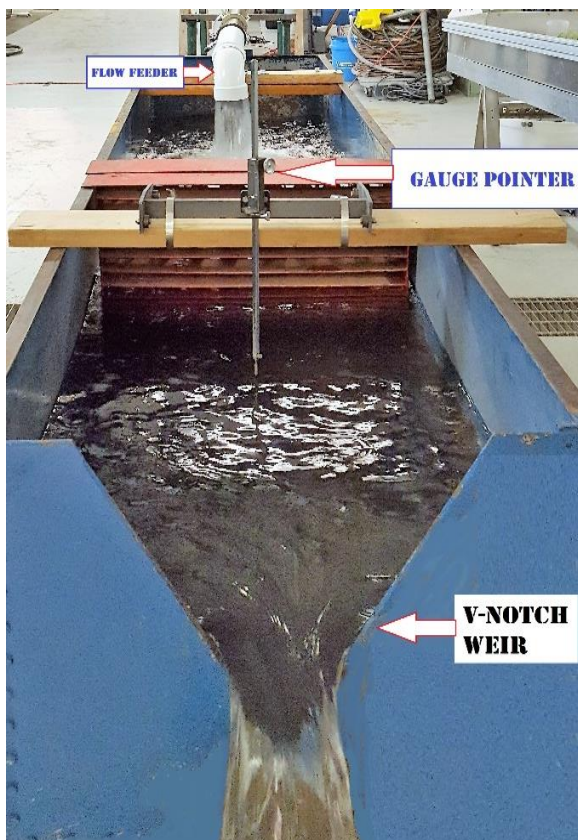


Figure 3. The experimental setup rig system

4. RESULTS AND DISCUSSION

The explicit numerical solution was established according to the four-point box partial differential outline principle. The steady flow hydrograph was employed as an upstream boundary condition, while the known water depth (stage hydrograph) was used as a downstream boundary condition. Thus, the water surface elevation value would be estimated as a result of the numerical solution of Eqns. (11) and (12) simultaneously. Figures 4-10 show the correlation between the simulated water surface profile and the observed profile during the set of discharges previously mentioned in Table 1.

The results of comparing the calculated practically water surface levels with those calculated by the proposed numerical method, presented in the previous Figures 4-10, showed a great convergence. However, in order to evaluate the performance of the relationship between the amount of observed water surface elevation over the weir and the calculated values by the explicit numerical solution, a Nash-Sutcliffe Error measurement was carried out based on the credibility and reliability of this methodology [22-24]. Eq. (13) represents the Nash-Sutcliffe Error, where h_{obs} is the measured quantity, h_{sim} is the mimic quantity, and \bar{h}_{obs} is the mean of the measured quantity.

$$NSE = 1 - \frac{\sum(h_{obs} - h_{sim})^2}{\sum(h_{obs} - \bar{h}_{obs})^2} \quad (13)$$

The range of the Nash-Sutcliffe error is from 1 to $-\infty$. If $NSE=1$, that means a great match of the mimicked to the measured variable. When the $NSE=0$, model forecasts are accurate to the average filed data. Finally, if the $NSE < 0$ indicates that the model simulation results are far from the average observed data.

Table 1 lists the value of NSE corresponding to each tested discharge in this study. It is noted that the average value of $NSE=0.975$ which is close to 1, indicating the high convergence between the values of the water level above the weir measured using the proposed explicit numerical model compared to the results obtained experimentally.

By observing the discharge of the water released, shown in Figures 4-10, over the weir used in this study, one can note that with the increase in the discharge values, there is a high agreement between the results obtained practically with those calculated theoretically. This is because an increase in the discharge will lead to an increase in the velocity head above the weir and, thus, an increase in the momentum force, making the water's surface push farther. On the other hand, as for the low discharges, it works to reduce the velocity head, which leads to a decrease in the momentum of the water and makes the curve of the water surface closer to the weir.

Table 1. The Nash-Sutcliffe error of the proposed approach

Test No.	Discharge (L/s)	NSE
1	10	0.984
2	20	0.996
3	30	0.996
4	40	0.976
5	50	0.962
6	60	0.962
7	70	0.952
Average NSE =		0.975

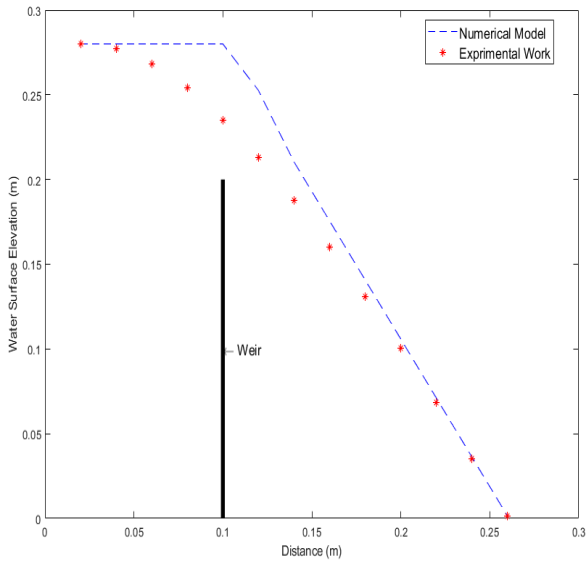


Figure 4. The shape of water surface profile flow=10 L/s

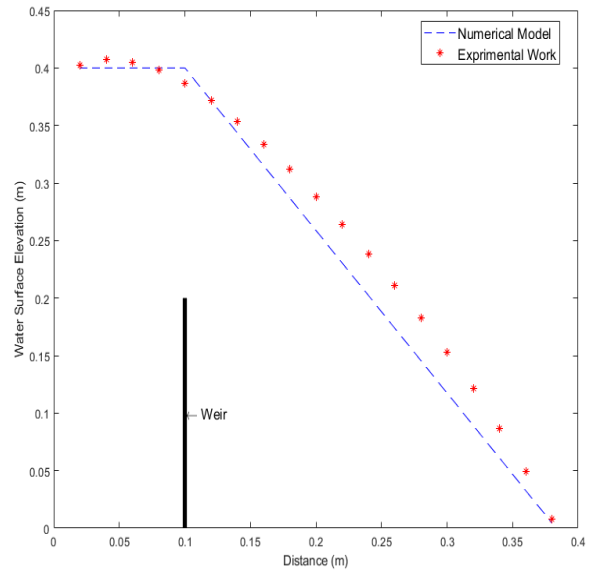


Figure 7. The shape of water surface profile flow=40 L/s

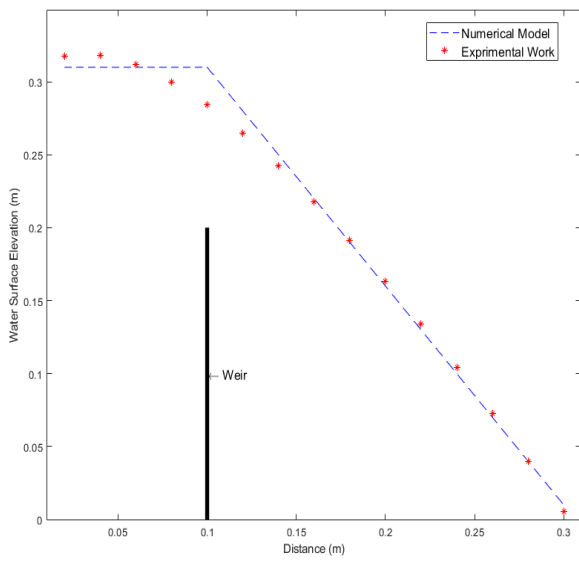


Figure 5. The shape of water surface profile flow=20 L/s

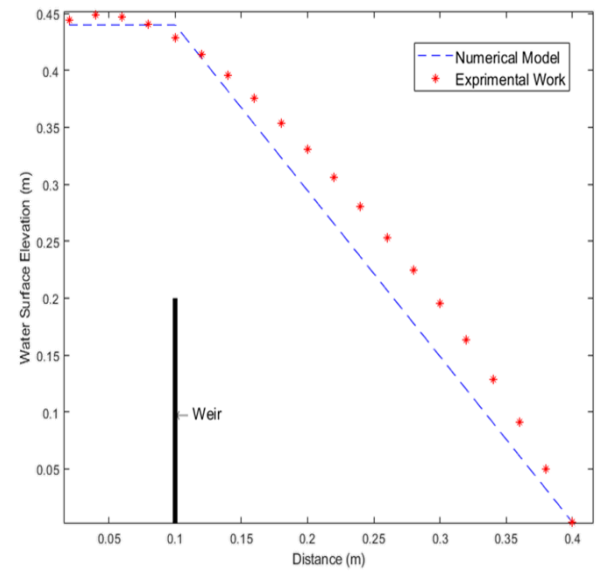


Figure 8. The shape of water surface profile flow=50 L/s

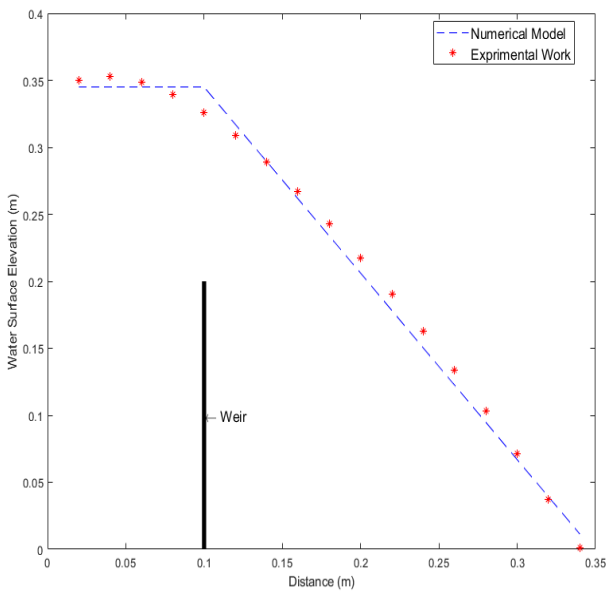


Figure 6. The shape of water surface profile flow=30 L/s

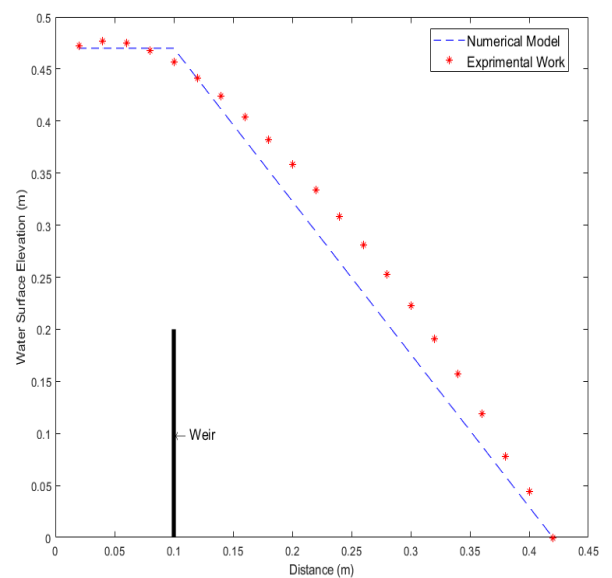


Figure 9. The shape of water surface profile flow=60 L/s

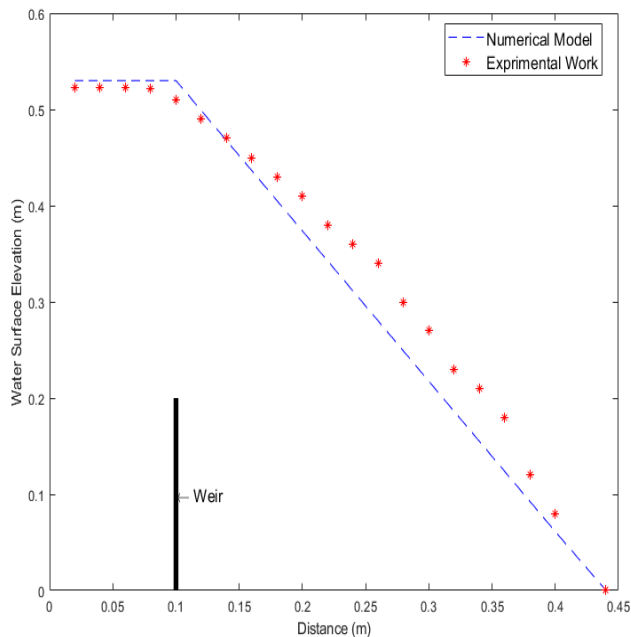


Figure 10. The shape of water surface profile flow=70 L/s

5. CONCLUSIONS

The water surface profile over the V-notch weir was measured both experimentally and numerically in this study. The results of this study indicate a high matching between the numerical model and experimental measurement. Speaking of that, the Nash-Sutcliffe error was calculated, and it was found that average NSE=0.975, which is very close to 1 and indicates a great ability of the model to mimic the experimental results. This will allow the opportunity for water resources engineers to have a tool that can predict the depth of the water during unexpected flow events.

Further investigations may be carried out for future work to express the validity of the proposed model with another types of weirs.

REFERENCES

- Li, J., Han, J. (2022). Experimental study of discharge formulas for rectangular sharp-crested weirs under free flow condition. *Flow Measurement and Instrumentation*, 84: 102115. <https://doi.org/10.1016/j.flowmeasinst.2021.102115>
- Fathi-moghaddam, M., Sadrabadi, M.T., Rahmanshahi, M. (2018). Numerical simulation of the hydraulic performance of triangular and trapezoidal gabion weirs in free flow condition. *Flow Measurement and Instrumentation*, 62: 93-104. <https://doi.org/10.1016/j.flowmeasinst.2018.05.005>
- Mohammed-Ali, W.S. (2012). Hydraulic characteristics of semi-elliptical sharp crested weirs. *International Review of Civil Engineering*, 3(1): 42-46.
- Khode, B.V., Tembhurkar, A.R., Porey, P.D., Ingle, R.N. (2012). Experimental studies on flow over labyrinth weir. *Journal of Irrigation and Drainage Engineering*, 138(6), 548-552. [https://doi.org/10.1061/\(ASCE\)IR.1943-4774.0000336](https://doi.org/10.1061/(ASCE)IR.1943-4774.0000336)
- Carollo, F.G., Ferro, V., Pampalone, V. (2012). Experimental investigation of the outflow process over a triangular labyrinth-weir. *Journal of Irrigation and Drainage Engineering*, 138(1): 73-79. [https://doi.org/10.1061/\(ASCE\)IR.1943-4774.0000366](https://doi.org/10.1061/(ASCE)IR.1943-4774.0000366)
- Hussain, R.A., Hassan, S.A., Jamel, A.A.J. (2022). Experimental study on flow over triangular labyrinth weirs. *International Journal of Design & Nature and Ecodynamics*, 17(2): 249-255. <https://doi.org/10.18280/ijdne.170211>
- Rao, S.S., Shukla, M.K. (1971). Characteristics of flow over weirs of finite crest width. *Journal of the Hydraulics Division*, 97(11): 1807-1816. <https://doi.org/10.1061/JYCEAJ.0003138>
- Aydin, M.C. (2012). CFD simulation of free-surface flow over triangular labyrinth side weir. *Advances in Engineering Software*, 45(1): 159-166. <https://doi.org/10.1016/j.advengsoft.2011.09.006>
- Woodburn, J.G. (1932). Tests of broad-crested weirs. *Transactions of the American Society of Civil Engineers*, 96(1): 387-416. <https://doi.org/10.1061/TACEAT.0004394>
- Tracy, H.J. (1957). Discharge characteristics of broad-crested weirs (Vol. 397). US Department of the Interior, Geological Survey. <https://doi.org/10.3133/cir397>
- Xu, T., Jin, Y.C. (2017). Numerical study of the flow over broad-crested weirs by a mesh-free method. *Journal of Irrigation and Drainage Engineering*, 143(9): 04017034. [https://doi.org/10.1061/\(ASCE\)IR.1943-4774.0001211](https://doi.org/10.1061/(ASCE)IR.1943-4774.0001211)
- Cassidy, J.J. (1965). Irrotational flow over spillways of finite height. *Journal of the Engineering Mechanics Division*, 91(6): 155-173. <https://doi.org/10.1061/JMCEA3.0000692>
- Mohammed-Ali, W.S., Khairallah, R.S. (2023). Flood risk analysis: The case of Tigris River (Tikrit/Iraq). *Tikrit Journal of Engineering Sciences*, 30(1): 112-118. <https://doi.org/10.25130/tjes.30.1.11>
- Ramamurthy, A.S., Tim, U.S., Rao, M.V.J. (1988). Characteristics of square-edged and round-nosed broad-crested weirs. *Journal of Irrigation and Drainage Engineering*, 114(1): 61-73. [https://doi.org/10.1061/\(ASCE\)0733-9437\(1988\)114:1\(61\)](https://doi.org/10.1061/(ASCE)0733-9437(1988)114:1(61))
- Mohammed-Ali, W.S. (2020). Minimizing the detrimental effects of hydro-peaking on riverbank instability: The lower Osage River case. *Missouri University of Science and Technology*.
- Mohammed-Ali, W.S., Khairallah, R.S. (2022). Review for some applications of riverbanks flood models. In *IOP Conference Series: Earth and Environmental Science*, 1120(1): 012039. <https://doi.org/10.1088/1755-1315/1120/1/012039>
- Lai, W., Khan, A.A. (2018). Numerical solution of the Saint-Venant equations by an efficient hybrid finite-volume/finite-difference method. *Journal of Hydrodynamics*, 30: 189-202. <https://doi.org/10.1007/s42241-018-0020-y>
- Szymkiewicz, R. (1991). Finite-element method for the solution of the Saint Venant equations in an open channel network. *Journal of Hydrology*, 122(1-4): 275-287. [https://doi.org/10.1016/0022-1694\(91\)90182-H](https://doi.org/10.1016/0022-1694(91)90182-H)
- Molinas, A., Yang, C.T. (1985). Generalized water surface profile computations. *Journal of Hydraulic Engineering*, 111(3): 381-397. [https://doi.org/10.1061/\(ASCE\)0733-](https://doi.org/10.1061/(ASCE)0733-)

- [20] Al-Juhaishi, E.H.K. (2020). Novel approaches for constructing persistent Delaunay triangulations by applying different equations and different methods. Doctoral dissertation, Missouri University of Science and Technology.
- [21] Mohammed-Ali, W.S. (2011). The effect of middle sheet pile on the uplift pressure under hydraulic structures. *European Journal of Scientific Research*, 65(3): 350-359.
- [22] Mohammed-Ali, W., Mendoza, C., Holmes, R.R. (2021). Riverbank stability assessment during hydro-peak flow events: The lower Osage River case (Missouri, USA). *International Journal of River Basin Management*, 19(3): 335-343.
- [23] Mohammed-Ali, W., Mendoza, C., Holmes Jr, R.R. (2020). Influence of hydropower outflow characteristics on riverbank stability: Case of the lower Osage River (Missouri, USA). *Hydrological Sciences Journal*, 65(10): 1784-1793.
- [24] Nash, J.E., Sutcliffe, J.V. (1970). River flow forecasting through conceptual models part I—A discussion of principles. *Journal of Hydrology*, 10(3): 282-290. [https://doi.org/10.1016/0022-1694\(70\)90255-6](https://doi.org/10.1016/0022-1694(70)90255-6)